# Carbon Monoxide Generation, Dispersion and Exposure from Indoor Operation of Gasoline-powered Electric Generators under Actual Weather Conditions

Liangzhu (Leon) Wang[1]
Steven J. Emmerich[2]
Andrew K. Persily[2]
Cheng-Chun Lin[1]

[1]Department of Building, Civil and Environment Engineering,
Concordia University
1455 de Maisonneuve Blvd. West, Montreal, Quebec, Canada H3G1M8

[2]Indoor Air Quality and Ventilation Group, Energy and Environment Division
Engineering Laboratory, National Institute of Standards and Technology
100 Bureau Drive Gaithersburg, MD 20899

Content submitted to and published by:
Building and Environment
Volume 56: 283-290
2012

U.S. Department of Commerce
*Dr. Rebecca M. Blank, Acting Secretary*

National Institute of Standards and Technology
*Patrick D. Gallagher, Director*

NIST National Institute of Standards and Technology • U.S. Department of Commerce

## DISCLAIMERS

Certain commercial entities, equipment, or materials may be identified in this document in order to describe an experimental procedure or concept adequately. Such identification is not intended to imply recommendation or endorsement by the National Institute of Standards and Technology, nor is it intended to imply that the entities, materials, or equipment are necessarily the best available for the purpose.

Any link(s) to website(s) in this document have been provided because they may have information of interest to our readers. NIST does not necessarily endorse the views expressed or the facts presented on these sites. Further, NIST does not endorse any commercial products that may be advertised or available on these sites.

## Abstract

Gasoline-powered electric generators are widely used during power outages such as those caused by hurricanes and winter storms. Based on currently available data, about 95 % of generator-related carbon monoxide (CO) fatalities were associated with operating carbureted, spark-ignited and gasoline-powered generators in enclosed spaces. To investigate the indoor CO exposure associated with running a generator indoors, the generation of CO was measured from a generator in an enclosed shed. Correlations of CO generation and $O_2$ consumption rates were developed as functions of $O_2$ level and actual generator load output. An indoor air quality and ventilation model was then used to predict the air change rates and CO levels in the shed, which were then compared with measured values. This study also used the simulation model to calculate CO generation and dispersion, and occupant exposures to CO, with a generator running in the garage of a house during weather conditions consistent with the days after Hurricane Katrina in the summer of 2005. For the simulation conditions, it was found that the resultant CO could reach dangerous levels in most rooms of the house about two hours after the generator started.

**Keywords**: carbon monoxide gasoline-powered generator, in situ experiments, carbon monoxide exposure, multizone.

## Nomenclature

| | |
|---|---|
| *%COHb* | carboxyhemoglobin in percentage |
| $[COHb]_t$ | ml of CO per ml blood at time t |
| $[OHb]_{max}$ | ml of $O_2$ per ml blood under normal conditions, ml/ml |
| $B$ | constant related to CO lung diffusivity, min·mm Hg/ml |
| $C_{CO}$ | CO concentration, ppm(v) |
| $C^*_{O_2}$ | non-dimensional $O_2$ concentration |
| $L_o$ | output load of a generator |
| $L^*_o$ | non-dimensional generator load |
| $M$ | ratio of affinity of blood for CO to that for $O_2$ |
| $n$ | total number of data points to be compared |
| $P_{CO}$ | partial pressure of CO in the inhaled air, mm Hg |
| $P_{O_2}$ | partial pressure of $O_2$ in the inhaled air, mm Hg |
| $RPM$ | revolutions per minute of the generator engine, $min^{-1}$ |
| $S_{CO}$ | CO generation rate, g/h |
| $S^*_{CO}$ | non-dimensional CO generation rate |
| $S_{CO,min}$ | minimum CO generation rate, g/h |
| $S_{CO,max}$ | maximum CO generation rate, g/h |
| $S_{m,i}$ | measured source for the data point $i$, g/h |
| $\overline{S_m}$ | average value of measured sources, g/h |

| | |
|---|---|
| $S^*_{O_2}$ | non-dimensional $O_2$ consumption rate |
| $S_{p,i}$ | predicted source for the data point *i,* g/h |
| $\overline{S_p}$ | average value of predicted sources, g/h |
| *t* | exposure time, min |
| $V_A$ | alveolar ventilation rate, ml/min |
| $V_b$ | blood volume, ml |
| $V_{CO}$ | Rate of endogenous CO production, ml/min |
| | |
| ***Greek Symbol*** | |
| Δ | difference |

## 1. Introduction

During power outages caused by natural disasters, such as hurricanes, tornadoes, floods, and winter storms, gasoline-powered electric generators are widely used in U.S. households. As a product of incomplete gasoline combustion, carbon monoxide (CO) causes significant safety and health concerns related to generator usage. From the years 1999 to 2008, 30 % of the power outage-related CO fatalities occurred mainly after hurricanes in September and ice/snow storms in January and December of 2005 [1]. During this period, there were 592 deaths caused by CO poisoning associated with the use of engine-driven tools in the U.S., 86 % of which were associated with gasoline-powered electric generators. Based on concerns about generator theft and noise to neighbors, and being unaware of the seriousness of CO hazards, users sometimes operate generators in an enclosed space, such as a basement, garage, shed, or crawlspace [2]. During the years 1999 through 2008, 95 % of the 422 generator-related CO fatalities, which are known to have occurred in or near the home, were found to be associated with operating generators indoors [1]. In the meantime, the possession of household generators in the U.S. has climbed in recent years, from an estimated 9.2 million units in 2002 to 10.6 million units in 2005 [2]. Based on these concerns the U.S. National Institute Standards and Technology (NIST) conducted a series of studies, funded by the U.S. Consumer Product Safety Commission (CPSC), of CO generation, dispersion and occupant exposure from generators operating indoors.

Ideally, CO generation from a generator engine would be determined from the stoichiometrics of gasoline combustion. However, this approach is not realistic for the following reasons. First, gasoline is not a homogeneous molecule but instead is typically a mixture of hydrocarbons with 6 to 12 carbon atoms, although gasoline is often simplified as isooctane ($C_8H_{18}$) for theoretical estimations [3]. The composition of gasoline also often varies with altitude, season and local emission regulations. The stoichiometric ratios of gasoline combustion would also vary due to specific air-fuel mixing ratio, gasoline composition, and engine operating conditions. Therefore, a theoretical determination of CO generation is impractical, and these generation rates must be measured experimentally.

To determine the rate of CO generation, CPSC researchers have conducted experiments on four commercially available generators with a rated load output of 0.9 kW to 5.55 kW in an enclosed experimental chamber [4]. They measured the levels of CO and oxygen ($O_2$), generator load output, air temperature and humidity, and calculated the CO generation rate at steady state. However, a generator will operate differently in actual homes due to the significantly different ambient conditions. First, the air change rates in the chamber tests ranged from 13 $h^{-1}$ to 29 $h^{-1}$, which are much higher than actual conditions in houses or garages. The estimated median infiltration rate of U.S. houses is 0.44 $h^{-1}$ based on an analysis of 266 houses [5]. At a lower air change rate, more CO is expected to be generated due to the shortage of $O_2$. Additionally, the CO generation in the chamber tests was also evaluated at steady state. In actual conditions, generator operation is a transient process due to the continual depletion of $O_2$ level and the variation of load and ambient weather conditions. Our literature search did not reveal previous studies on CO generation from generators in real conditions, where $O_2$ levels can become significantly lower than ambient, and thereby impact CO generation. Previous studies on indoor CO generations were mostly on tailpipe emissions from vehicles [6-8], most of which are equipped with emission control devices. Limited studies were found on the CO generation, transport and exposure from indoor operation of generators, which often do not have emission controls, under the conditions of depleted $O_2$ and real weathers.

In this paper, we report on the generation, dispersion and exposure of CO from one of the CPSC tested generators based on both experimental and simulation methods. A series of tests were conducted in a single-zone shed under variable weather conditions to measure levels of CO and $O_2$ [9]. The transient CO generation rates and $O_2$ consumption rates were calculated. We then developed an empirical correlation of CO generation rate versus $O_2$ level as the CO source model, which was validated against the measured data in the single-zone shed. Numerical simulations were used to determine the CO dispersion and occupant exposure in multi-zone residential homes by using a multizone indoor air quality analysis software, CONTAM [10]. Using the empirical model of CO generation, we modeled a generator running in a garage of a typical US single-family house. The weather conditions of New Orleans, Louisiana after Hurricane Katrina in September 2005 were selected for the simulation. CO levels and occupant CO exposures were predicted in different rooms of the house. This paper provides a quantitative description of the amount of CO generated, its dispersion, and resultant hazards when operating a generator indoors under actual weather conditions.

## 2. Experimental study

Measurement of CO generation rates from an actual generator was used to develop a model of the CO source strength for use in computer simulations and other analyses. The generation of CO is a function of various parameters, including the $O_2$ level, electrical loading on the generator, air temperature, and possibly moisture [4]. The $O_2$ level and air temperature in an enclosed space are directly affected by air change rate of the space and indirectly by ambient weather conditions, e.g. wind speed and direction, which impact the air change rate. The goal of these measurements was to develop correlations of CO generation and $O_2$ consumption rates with these factors.

### 2.1 Experimental setup

A currently marketed, carbureted spark-ignited gasoline-powered portable generator was tested in a single-zone shed as shown in Figure 1. The shed is an enclosed space with dimensions of approximately 4.88 m (L) × 3.05 m (W) × 2.90 m (H). The generator, which has a full-load power rating of 5.5 kW, was placed on a platform in the middle of the shed. Approximately 40 % of portable generators purchased by consumers between 2003 and 2005 were in the power output range from 5.0 kW to less than 6.5 kW [2]. A portable AC-powered load bank, which can be manually set to a maximum value of 10 kW in steps of 250 W, was located outside the shed and used to apply an electrical load on the generator. Air sample lines were placed in the center of the shed (middle from the walls and from the floor) for measuring CO, $O_2$, and sulfur hexafluoride ($SF_6$) concentrations. A non-dispersive infrared CO analyzer, a portable magneto-dynamic $O_2$ analyzer, and a gas chromatograph with an electron capture detector were used to measure the respective concentrations of these three gases. The air temperature and humidity in the shed were measured at two locations near two sidewalls of the shed. The air change rate was measured using the tracer gas decay method [11]. A pulse of $SF_6$ was injected for about two to three minutes at a central location in the shed, about three quarters above the shed floor, to measure the air change rates of the shed by using the tracer decay method. The measured gas concentration, air temperature, and humidity were recorded remotely by a data acquisition system. Note that the shed was naturally ventilated and there was no mechanical system, e.g. exhaust opening or duct, to directly evacuate the flue gases during the operation of the generator. The detailed experimental setup and uncertainty analysis can be found from Wang et al. [9].

Figure 1. Generator installed in the single-zone shed.

### 2.2 Experimental results and analysis

Table 1 provides a summary of test results and corresponding weather conditions for four tests with the load bank set at 2.5 kW and four tests at 5.0 kW. Within less than two hours, the CO level reached its maximum level: 27500 mg/m$^3$ in Test 1 and 9400 mg/m$^3$ in Test 4. To put these values in context, the immediately dangerous to life or health (IDLH) value of CO is 1380 mg/m$^3$ [12]. Simultaneously, $O_2$ decreased from the ambient level of about 20.9 % to about 17 % (i.e., 80 % of the initial level) in most of the tests.

Table 1. Summary of test results in a shed and ambient weather conditions.

| Test | Elec. Load Setting (kW) | Run Time (min) | Weather Condition | | Shed Air Temp. (°C) | Air Change Rate ($h^{-1}$) | Max. CO ($mg/m^3$) | Min. $O_2$ (%) (vol.) |
|---|---|---|---|---|---|---|---|---|
| | | | Avg. Temp. (°C) | Avg. Wind Velocity (m/s) | | | | |
| 1 | 2.5 | 86 | 15.6 | 1.1 | 32 to 50 | 2.6 | 27500 | 16.9 |
| 2 | | 101 | 17.2 | 2.1 | 30 to 53 | 3.1 | 26800 | 16.8 |
| 3 | | 80 | 13.8 | 1.3 | 32 to 52 | 2.9 | 23100 | 17.1 |
| 4 | | 106 | 4.0 | 2.3 | 15 to 43 | 3.6 | 9400 | 18.2 |
| 5 | 5.0 | 62 | 7.9 | 3.6 | 12 to 44 | 3.7 | 24500 | 17.4 |
| 6 | | 74 | 13.7 | 2.2 | 24 to 51 | 2.9 | 23100 | 17.1 |
| 7 | | 65 | 8.1 | 3.1 | 17 to 41 | 3.0 | 25800 | 16.9 |
| 8 | | 66 | 8.6 | 2.3 | 24 to 45 | 3.6 | 25600 | 17.0 |

Based on these data, a correlation of transient CO generation rate, $O_2$ consumption rate, and the actual (measured) generator load output was developed using a non-commercial statistical analysis software package, R [13], which is a GNU project with its source code freely available under the GNU General Public License. The correlations are expressed as follows [9]:

$$S^*_{CO} = e^{-1.3504 C^*_{O_2} + 2.43738 L^*_o - 0.99583} - L^*_o \qquad (1)$$

$$S^*_{O_2} = e^{0.64191 C^*_{O_2} - 0.06588 L^*_o - 0.1939} - L^*_o \qquad (2)$$

$$L^*_o = 4.121 (C^*_{O_2})^3 - 8.0424 (C^*_{O_2})^2 + 5.3478 C^*_{O_2} - 0.2307 \qquad \text{(for 5.0 kW)} \qquad (3)$$

where the non-dimensional parameter, $S^*_{CO}$, is defined by

$$S^*_{CO} = \frac{S_{CO} - S_{CO,min}}{S_{CO,max} - S_{CO,min}} \qquad (4)$$

so that $0 \le S^*_{CO} \le 1$. The $S_{CO,min}$ and the $S_{CO,max}$ values are the minimum and maximum five-minute averaged CO generation rate, respectively. Similar definitions apply to the other non-dimensional parameters $S_{O_2}$, $C_{O_2}$, and $L_o$. Eq. (3) calculates the actual load output for the generator set at 5.0 kW. When the load is set at other levels, such as 2.5 kW, a similar correlation of Eq. (3) and the same simulation method as that of 5.0 kW can be applied.

Figure 2 shows the CO generation and $O_2$ consumption rates obtained from the tests compared to the prediction using Eqs. (1) and (2) for tests 4, 7 and 8. Generally, the correlations agree well with the measured data. Figure 2(a) also shows that the measured CO rates in this study are close to those of the CPSC [4], although their tests only obtained data for higher $O_2$ levels (>19 %) inside a test chamber. The normalized mean square error (NMSE) (ASTM E-741-00 2008) as defined by Eq. (5) can be used to compare the measured and predicted values. The NMSE value is about 8 % for the correlation of CO generation rate and 1 % for the predicted $O_2$ consumption rate. Some discrepancies were observed for oxygen levels over 18 % when the generator was set at a load of 5.0 kW.

$$\text{NMSE} = = \frac{1}{\overline{S_p}\,\overline{S_m}}\left[\frac{1}{n}\sum_{i=1}^{n}(S_{p,i} - S_{m,i})^2\right] \qquad (5)$$

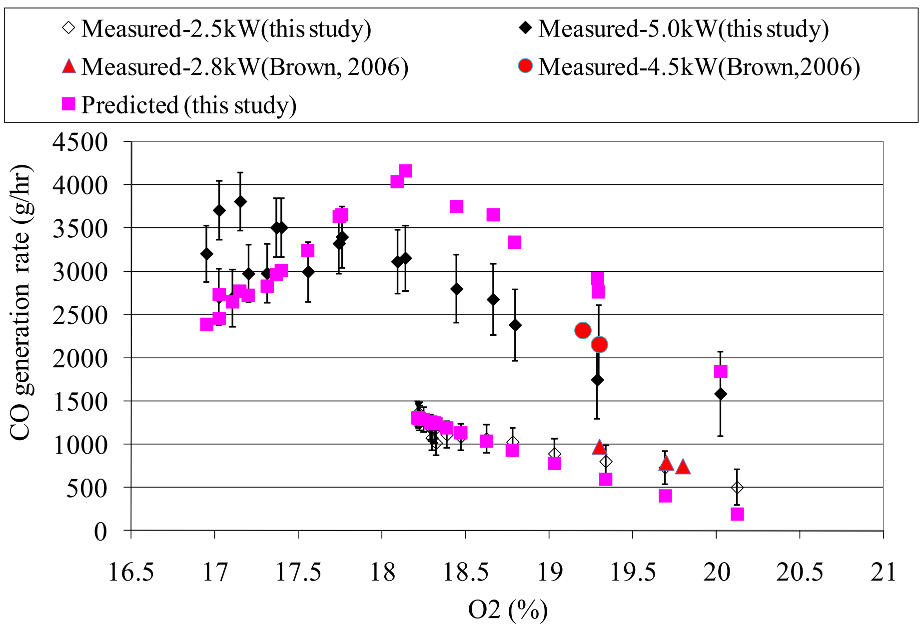


Figure 2(a).

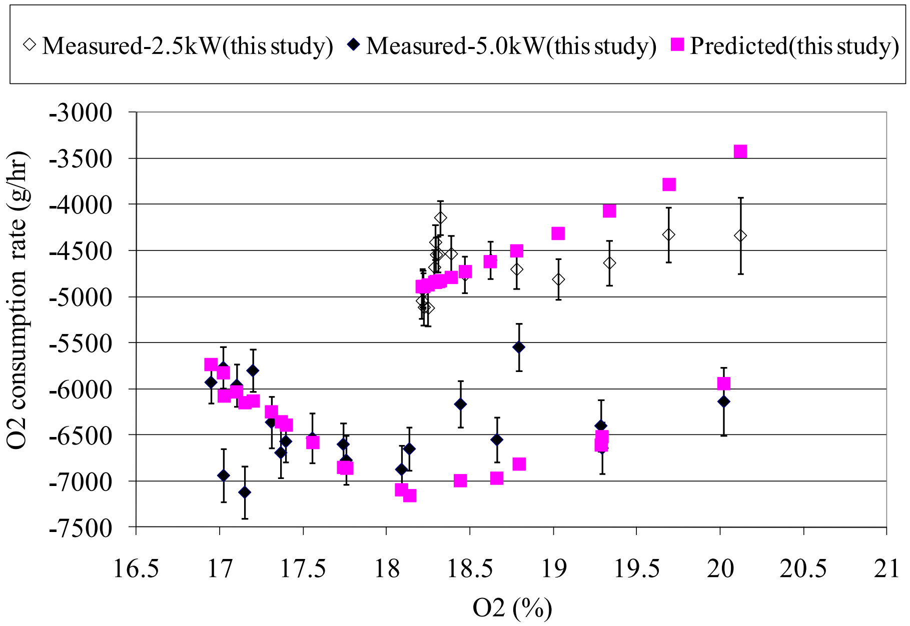


Figure 2(b).

Figure 2. Comparison of measured and predicted (a) CO generation rate, and (b) $O_2$ consumption rate as a function of $O_2$ level in the shed. Error bars show the uncertainty for each data point with a confidence level of 95 %.

As expected, the CO generation rate was also found to be a function of the surrounding $O_2$ level and generator load. Generally, a higher load or a lower $O_2$ level increases CO generation. Furthermore, the dependence of CO generation on $O_2$ level is non-linear. When $O_2$ is sufficiently low, as shown by the solid dots when the load was set at 5.0 kW, the CO generation started to decrease at a certain point during the tests. This decrease occurred because the $O_2$ level was too low to sustain effective gasoline combustion. Under these conditions, the generator tended to perform poorly: decreased rotation speed of the engine, clicking noises, vibrations, and reduced electrical output. The actual output is quantified by the correlation in Eq. (3) as a function of surrounding $O_2$ level. It was observed that the actual load output reduced to zero when the $O_2$ level was around 16.4 %, although the load was set to 2.5 kW or 5.0 kW. At this point in a test, the generator was generally shut down manually to prevent damage. In this study, an $O_2$ level of 16.4 % was referred to as the break-down $O_2$ level, at which point the generator stopped functioning. The correlations in Eqs. (1) and (2) will be used as source/sink strength models in the simulation studies described later in this paper.

## 3. Validation of the pollutant dispersion model

A CONTAM model was created to evaluate predictions of the test shed air change rates as well as CO and $O_2$ concentrations under transient conditions for the tests in Table 1. The latter validation effort is intended to evaluate the reliability of the correlations in Eqs. (1) through (3).

### *3.1 CONTAM simulation of a single zone*

Figure 3 shows the shed model in the CONTAM sketchpad interface. The generator was simulated as a source to account for CO generation and as a sink for $O_2$ consumption. The strength of the source/sink can be defined by two methods. One is the "super node method", which implements the correlations of Eqs. (1) through (3) using a group of control nodes. In CONTAM, a control node is a node generating output data/signal based on certain input data/signals using standard mathematical and logical functions. For example, the first term in the right hand side of Eq. (1) can be expressed by an exponent control node in CONTAM with the exponential term as an input. A super control node is a control network, which consists of a group of control nodes, links, and sensors that define a more complex equation or correlation. In this study, the input signals/parameters of the super control node are the $O_2$ level and the actual load output of the generator under transient conditions.

The second method is the "source schedule method", which simply defines the transient CO generation and $O_2$ depletion rates, and the generator actual load output, using a time schedule. The "source schedule method" uses the time-dependent measured data directly and is therefore expected to be more accurate than the super-node method. However, the super-node method is more generalizable as the measured generation and depletion data will not necessarily be available for other cases. Both methods are used here to validate the shed simulation model. In this study, outdoor levels of CO and $O_2$ were considered to be zero and 20.9 %, respectively.

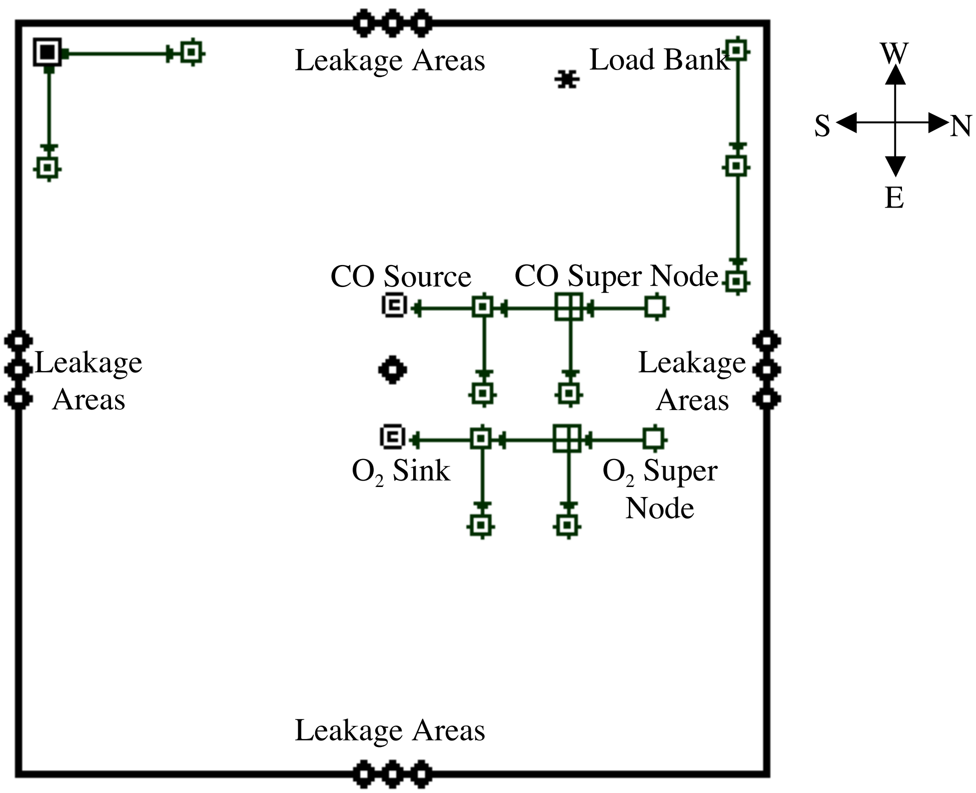


Figure 3. CONTAM model of the generator in the single-zone shed.

### *3.2 Validation of air change rates*

The first validation effort focused on the shed airflow model used in the simulations, because the predicted air change rate affects the prediction of CO and $O_2$ levels. Shed air leakage was measured with a blower door test [11]. The measured effective leakage area (ELA) used in the simulations was 7.5 $cm^2/m^2$ at a reference pressure of 4 Pa. The CONTAM airflow model was validated based on the predictions of air change rates. The air change rate prediction used the hourly-averaged weather data measured locally at the shed. A wind pressure coefficient profile [14] was used to define the coefficients at shed leakage paths. Figure 4 compares the predicted air change rates for the eight tests in Table 1 to the measured values. The calculated and predicted air changes generally agreed within the experimental uncertainty, which was roughly 10 % for a confidence level of 95 %.

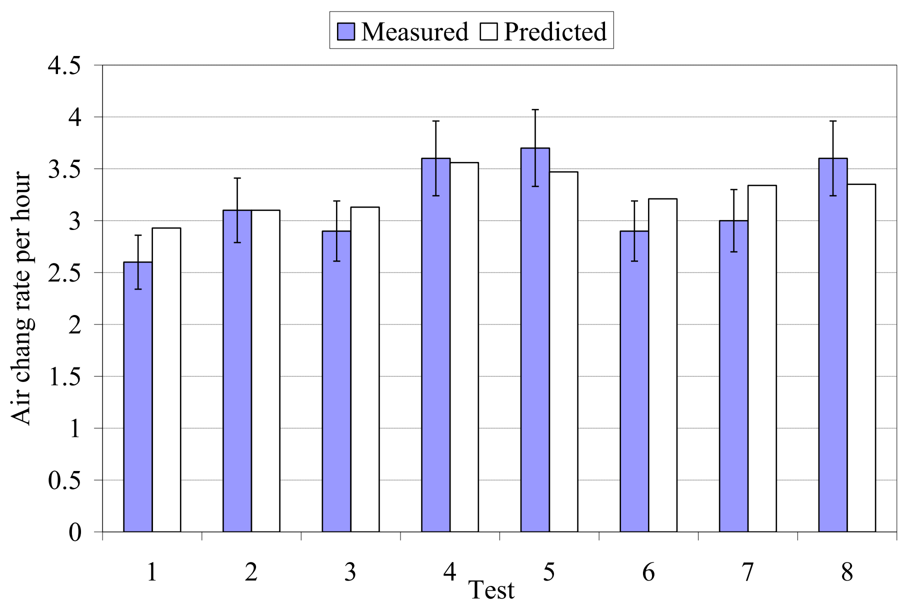


Figure 4. Comparison of measured and predicted shed air change rates.

### *3.3 Validation of transient CO and $O_2$ levels*

The predicted CO and $O_2$ levels are compared with the measured data for the generator load set at 5.0 kW. As discussed previously, the source schedule method used the measured data directly as inputs while the super node method models the CO generation and $O_2$ consumption using the correlations in Eqs. (1) through (3). Although the actual load outputs were only measured for Tests 4, 7 and 8, the super node method using Eqs. (1) through (3) performs reasonably well for Tests 5 and 6, where the load output data are not available, as illustrated by Figures 5(a) and 5(b). Figure 5(c) and 5(d) show that the source schedule method performed better than the super node method for Tests 7 and 8. The NMSE of the CO prediction defined by Eq. (5) in both cases is

8 % with the super node method whereas it is 2 % in Test 7 and 1 % for Test 8 with the source schedule method. For Test 7, the super node method significantly underestimated the CO level around the $O_2$ of 17 %. This discrepancy exists because the predicted CO source strength is less than the measured data for low oxygen levels (the data points near 17 % $O_2$ in Figure 2(a)). Similar reasoning applies to the $O_2$ concentration prediction. Note that the results of using the source schedule method for Tests 5 and 6 are similar to those of Tests 7 and 8, which are not shown here for simplification. Given that measured rates of CO generation and $O_2$ consumption are often not available, the super node method will become very useful. This can be demonstrated by the following analysis, in which the super node method was employed to model CO generation and dispersion in a house with multiple rooms/zones.

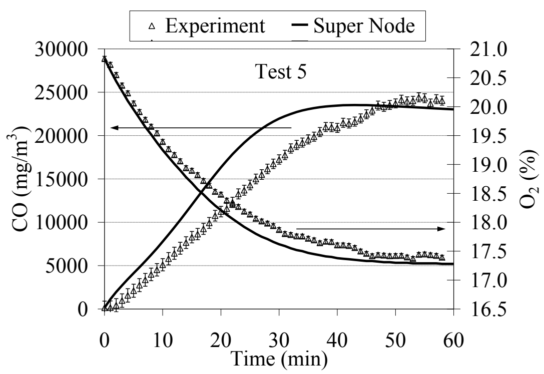


Figure 5(a) Test 5
$NMSE_{CO}$ = 8 %, $NMSE_{O2}$ = 2 %
(Super Node method)

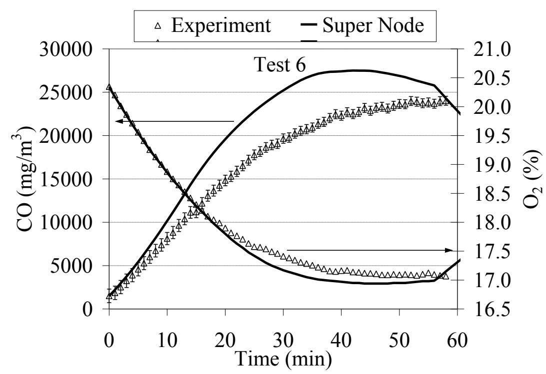


Figure 5(b) Test 6
$NMSE_{CO}$ = 4 %, $NMSE_{O2}$ = 0.1 %
(Super Node method)

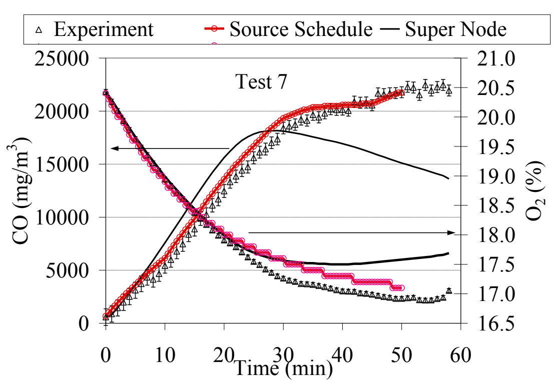


Figure 5(c) Test 7
$NMSE_{CO}$ = 8 %, $NMSE_{O2}$ = 0.1 %
(Super Node method);
$NMSE_{CO}$ = 2 %, $NMSE_{O2}$ = 0.1 %
(Source Schedule method)

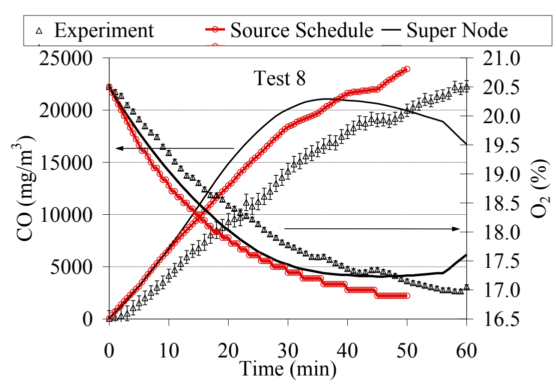


Figure 5(d) Test 8
$NMSE_{CO}$ = 8 %, $NMSE_{O2}$ = 0.1 %
(Super Node method);
$NMSE_{CO}$ = 1 %, $NMSE_{O2}$ = 0.1 %
(Source Schedule method)

Figure 5. Comparison of predicted and measured $O_2$ and CO levels in Tests 5 through 8. Error bars show the uncertainty for each experimental data point with a confidence level of 95 %.

## 4. Application to a full-scale residence

In order to investigate the application of these calculation methods to a realistic scenario, simulations were conducted for a single family house using weather data for New Orleans, LA during September 6$^{th}$ to September 7$^{th}$, 2005, a week after Hurricane Katrina. The weather conditions were obtained from the U.S. National Oceanic and Atmospheric Administration (NOAA) for a weather station located ten miles south of the city. Although real weather conditions were used, the modeled house was a generic house and does not correspond to any specific building.

### *4.1 CONTAM model of single family house*

Figure 6 shows the CONTAM representation of a two-story single family house with four bedrooms upstairs and an attached garage. A 5.5 kW generator, corresponding to the unit tested in the shed, was located in the garage to provide power to the house. The central air conditioning (AC) system was not operated during the simulations and the windows were assumed to be closed. The simulated time period was 8 h, from 22:00 Sept. 6$^{th}$, 2005 to 06:00 Sept. 7$^{th}$, 2005, when the occupants would presumably be sleeping. Hourly weather data were used in these simulations. The outdoor temperature was between 24 ˚C and 28 ˚C and the wind speed ranged from 0.4 m/s to 0.8 m/s with a wind direction of 10˚ through 30˚ relative to the north. The area-averaged effective leakage area (ELA) at the reference pressure of 4 Pa was 2.46 cm$^2$/m$^2$ for the house and 4.3 cm$^2$/m$^2$ for the garage, based on measured data in five residences with attached garages [15]. The CO source, $O_2$ sink strength, and actual load output of the generator were modeled by Eq. (1), (2), and (3), respectively, using the super node method as illustrated by the network of control nodes shown in the garage zone in Figure 6(a).

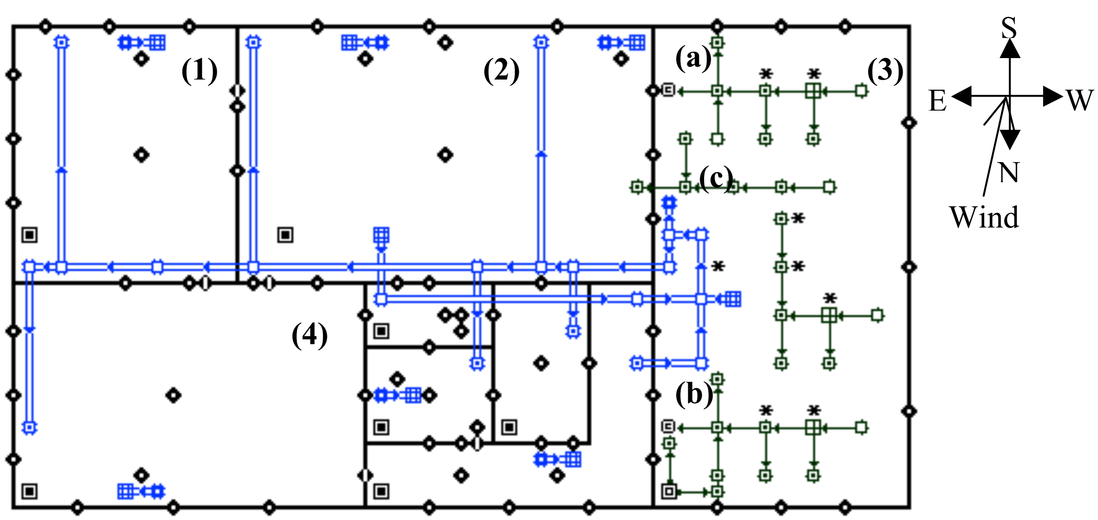


Figure 6(a)

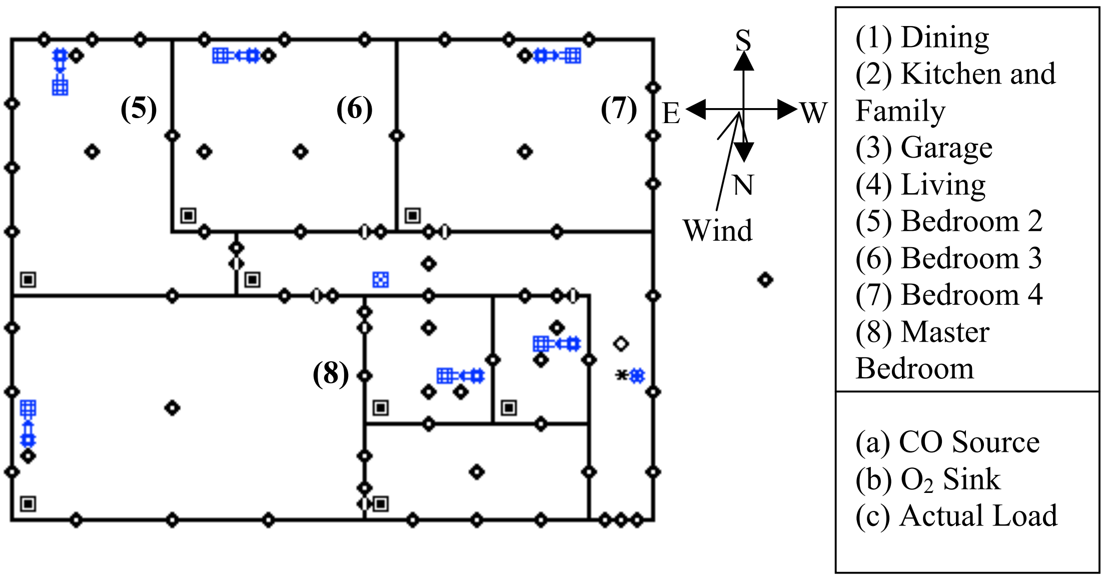


Figure 6(b)

Figure 6. CONTAM simulation model of (a) 1st and (b) 2nd floors of a house in New Orleans, LA.

## *4.2 Personal exposure model*

Carbon monoxide hazards to humans can be quantified by comparison to personal exposure guidelines or more complex exposure calculations. The CO threshold limit value (TLV) for an eight-hour exposure is 25 ppm(v) (29 mg/m$^3$) as promulgated by the American Conference of Governmental Industrial Hygienists [16]. The immediately dangerous to life or health (IDLH) level, which is based on the effects that might occur as a consequence of a 30-minute exposure, is 1200 ppm(v) (1,380 mg/m$^3$) for CO [12]. More detailed CO exposure measures can be calculated using the percentage of carboxyhemoglobin (*%COHb*) level that relates CO exposure to clinical symptoms [17]. One of the most popular models for *%COHb* is the Coburn-Foster-Kane (CFK) model, which has been broadly used and validated [18-20]. The CFK model takes into account important variables such as exposure duration, alveolar ventilation, partial pressure of CO in the inhaled air, blood volume, diffusivity of the lung for CO, and rate of endogenous CO production [21]. Eq. (5) and (6) show the integral form of the CFK equation [19].

$$[COHb]_t = [COHb]_{t-1} + \left(\frac{V_{CO}}{V_b} - \frac{[COHb]_{t-1} P_{O_2}}{MBV_b([OHb]_{\max} - [COHb]_{t-1})} + \frac{P_{CO}}{BV_b}\right)\Delta t \qquad (5)$$

$$[\%COHb]_t = \frac{[COHb]_t}{[OHb]_{max}} \times 100 \qquad (6)$$

where $P_{CO}$, partial pressure of CO in the air inhaled (mm Hg), was determined by $P_{CO} = C_{CO}/1316$ , in which $C_{CO}$ is the CO concentration in ppm(v). The initial $[COHb]_0$ is typically $1.659 \times 10^{-3}$ ml/ml for a non-smoker, which is equivalent to a $[\%COHb]_0$ of 0.75 % [19]. Table 2 relates *%COHb* levels to clinical symptoms of CO poisoning [17].

Table 2. Clinical symptoms of CO exposure as related to *%COHb*.

| *%COHb* | **Symptoms** |
|---|---|
| 0.4 to 1 | Normal physiological value for non-smokers; no perceptible effects |
| 2.5 to 3 | Decreased exercise performance for patients with angina |
| 4 to 5 | Increased symptoms for traffic policemen (headache and lassitude); increased oxygen debt in non-smokers |
| 5 to10 | Changes in myocardial metabolism and possible impairment; statistically significant diminution of visual perception, manual dexterity or ability to learn |
| 10 to 20 | Mild headache/possible tightness across the forehead, labored breathing, decreased exercise tolerance; impairment of time interval discrimination, visual acuity; manual coordination |
| 20 to 30 | Throbbing/decided headache; mild nausea, easy fatigability |
| 30 to 40 | Severe headache dizziness, vomiting, cognitive impairment; disturbed judgment, dimness of vision |
| 40 to 50 | Unconsciousness, coma, respiratory failure; fainting upon exertion; possible death from severe cellular hypoxia for prolonged exposure |
| 50 to 70 | Coma, brain damage, seizures; death |
| >70 | Typically fatal |

### *4.3 Results and discussion*

To illustrate the predicted performance of the generator in this study, Eqs. (1) and (2) are plotted in Figure 7 for an $O_2$ range of 16 % to about 20.9 % and an output load of 0 kW to about 5 kW. Based on the limited range of data for developing these correlations, we differentiate the range of measured data in Figure 7 using shading with extrapolated data unshaded. The curve with arrows shows the modeled generator operation from the starting point, **A** (22:00 Sept. 6$^{th}$, 2005) to the end **E** (06:00 Sept. 7$^{th}$, 2005), when the generator load was set to be 5.0 kW initially. Figure 7(a) shows that in the first ten minutes (from **A** to **B**), the load decreased significantly from a slight decline of oxygen level of 0.6 %. During the next forty minutes (from **B** to **C**), a similar decrease in load accompanied a significant reduction of 2.2 % in the $O_2$ level. Therefore, the generator operation curve from **A** to **B** moved downward indicating a decrease of CO generation rate but upward resulting in a huge increase of CO generation from **B** to **C**. Both the CO generation and $O_2$ depletion rates reached their peak values at the time **C.** During the seventy-five minutes, the generator load decreased significant to around 3500 W. At the time **D**, the garage $O_2$ reached the generator break-down level of 16.4 %, at which point the generator suffers a significant decrease in performance and stopped running, which corresponds to point **E**. Similar analysis applies to the $O_2$ usage rate in Figure 7(b).

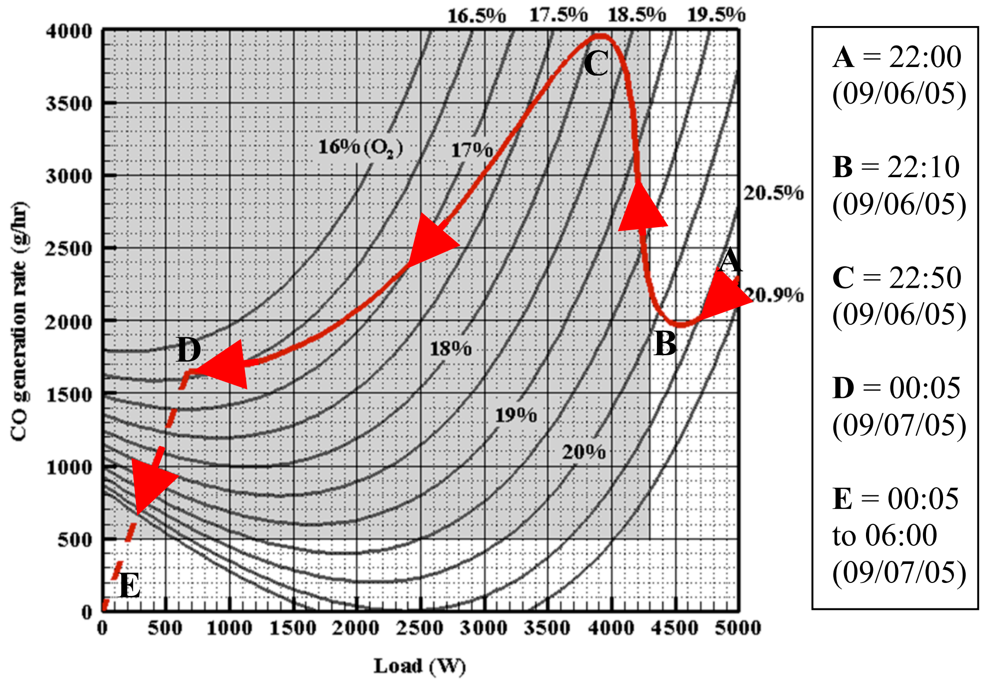


Figure 7(a)

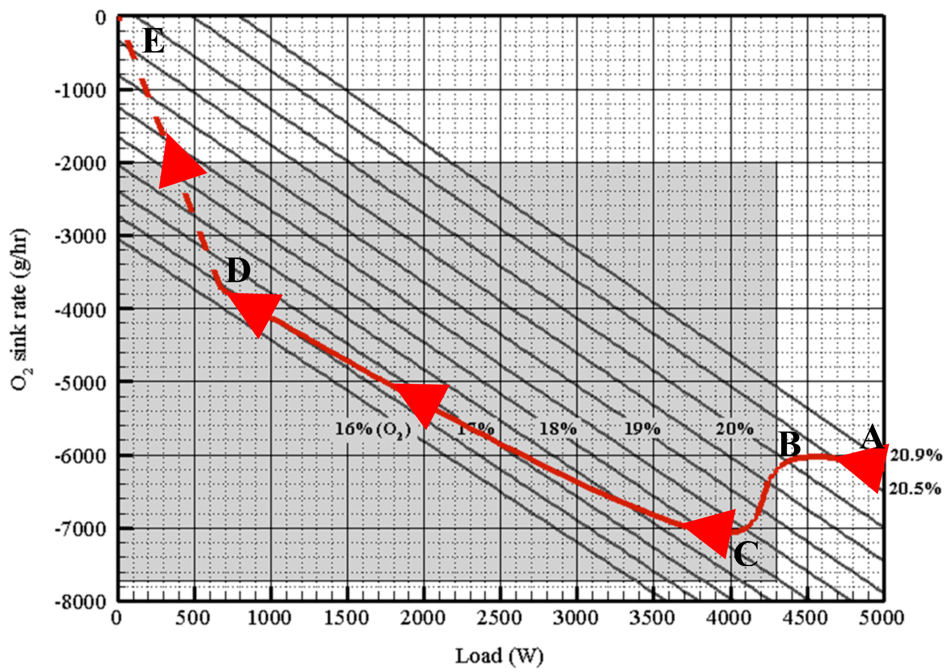


Figure 7(b)

Figure 7. Predicted (a) CO generation rate (g/h) and (b) $O_2$ consumption rate (g/h) as a function of generator output loads and $O_2$ levels (the shaded area is for the range of measurement data; the line is for the performance curve of the modeled generator).

The variations of the predicted CO and $O_2$ source terms in the garage caused variations of the CO levels in the house as shown in Figure 8. The house CO reached the ACGIH TLV level of 29 $mg/m^3$ at about 23:05 and remained well above the TLV during most of the test. Although the garage CO level started to decrease after the shutdown of the generator at 00:05, Sept. 7th, CO still increased in all bedrooms and started to decay around 04:00. At the end of the eight-hour simulation, the CO in all rooms of the house was still much higher than the TLV value.

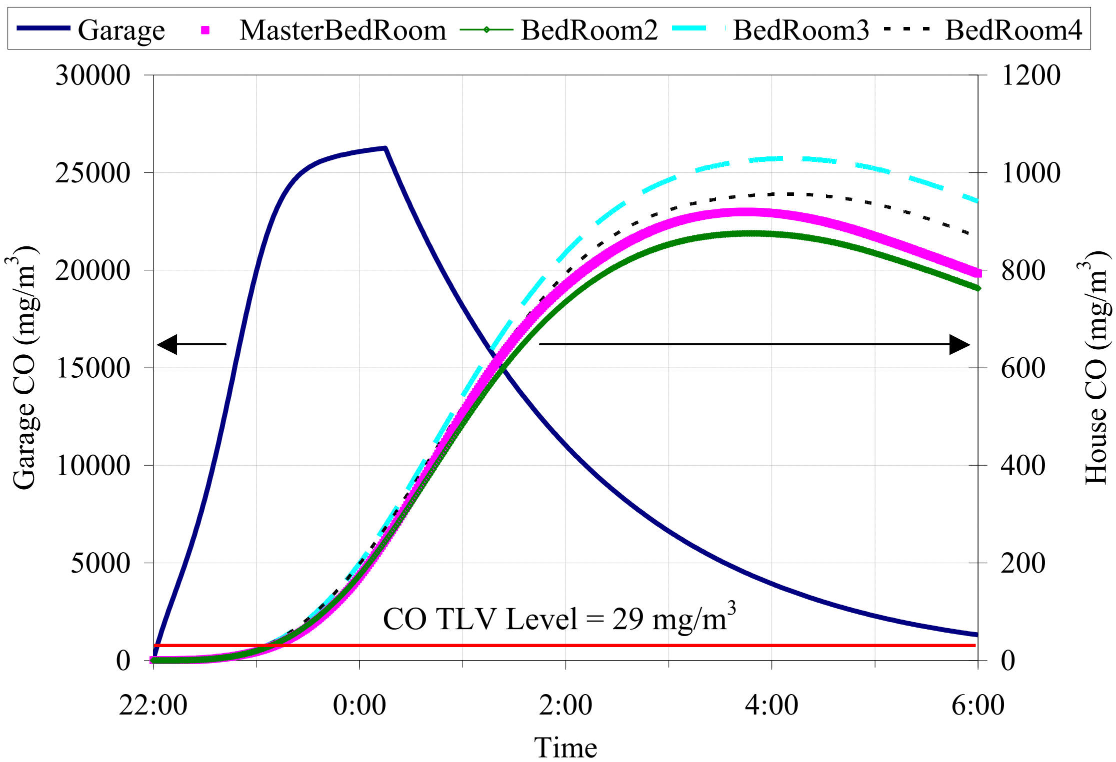


Figure 8. Predicted CO levels at different rooms/zones of the single family house.

The CFK model can be used to predict the levels of *%COHb* for people in different rooms of the house. Figure 9 illustrates that the *%COHb* level of 40 %, corresponding to serious health impacts as shown in Table 2, was reached in Bedroom 3 shortly after 02:00, but later for the rest of the bedrooms. Between 02:00 and 6:00, when the generator was no longer operating, and the *%COHb* remains above 40 % in all rooms for the remainder of the simulation period, with a maximum level of close to 60 %. In addition, relative to the level of 30 %, at which an occupant starts to feel headache from Table 2, it only took about 30 minutes in all rooms to increase from 30 % to 40 %, which leaves little time for people to take action. Note that although the simulations in this study used real experimental data and weather conditions as inputs, the results are only meant to illustrate the potential severity of CO levels when running a generator. In reality, scenarios could be more complex and the specific results from these simulations should not be used for other purposes such as risk assessments or forensic investigations.

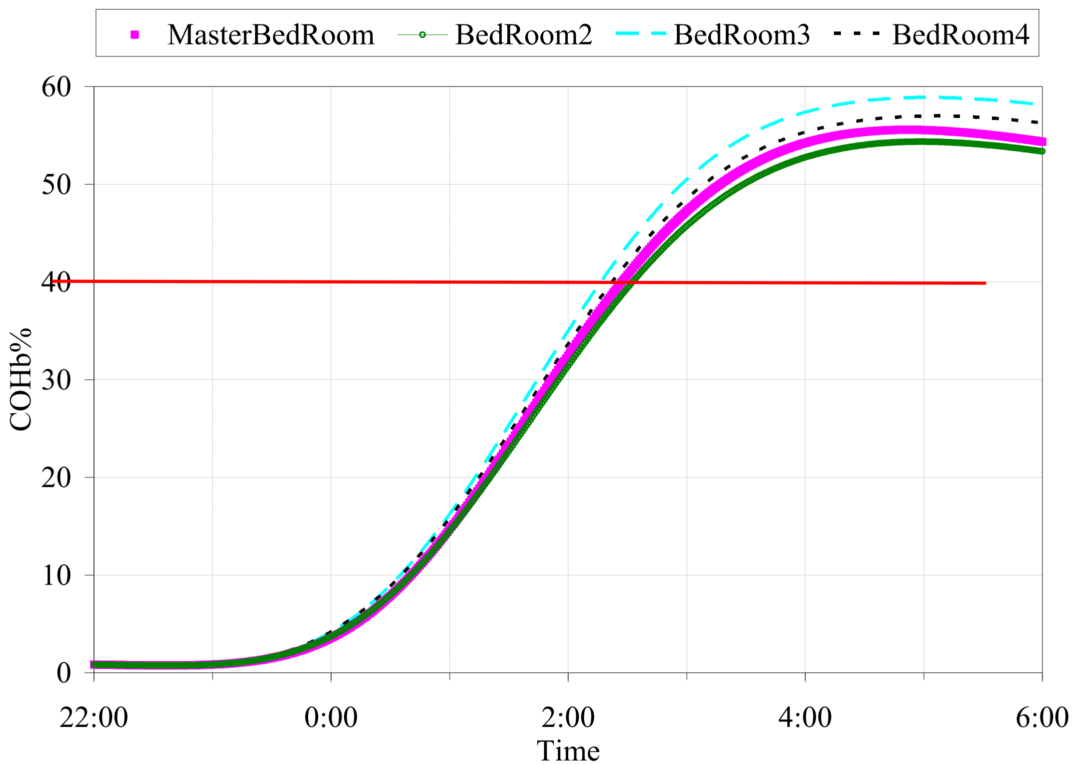


Figure 9. Predicted *%COHb* levels in the bedrooms of the single family house (the red line indicates the *%COHb* of 40 %, when a fatality of CO exposure may occur).

## 5. Conclusions

This paper addresses CO generation from gasoline-powered electric generators and its dispersion in enclosed single and multizone spaces. Eight experiments were conducted in a single zone shed to develop correlations of CO generation and $O_2$ consumption with $O_2$ level and actual load output of the generator. The shed was then modeled using the indoor air quality and ventilation analysis software, CONTAM. The predicted air change rates and CO and $O_2$ levels generally agreed well with the experimental data with some discrepancies for the generator load set at 5.0 kW. The correlations of CO source and $O_2$ sink strength were found to be applicable to modeling a generator running in enclosed spaces.

To demonstrate the CONTAM model, CO generation and dispersion were simulated in a single family house using weather conditions in New Orleans, LA during the aftermath of Hurricane Katrina in the summer of 2005. It was found that the CO level in the house could reach and remain significantly above the threshold limit value (TLV) for an eight-hour exposure. An analysis of predicted *%COHb* levels revealed that the levels for the house occupants could reach a lethal range around four hours after the generator started for the case simulated. It only took about thirty minutes for the *%COHb* level to increase from a symptomatically yet non-lethal level to a lethal level.

## Acknowledgments

This research was supported by the U.S. Consumer Product Safety Commission (CPSC) under the interagency agreement CPSC-I-06-0012 between the U.S. Consumer Product Safety Commission and the National Institute of Standards and Technology (NIST). The authors would like to thank Donald W. Switzer, Janet Buyer, Christopher J. Brown, and Susan Bathalon of CPSC, W. Stuart Dols and Gregory T. Linteris of NIST and Qingyan (Yan) Chen of Purdue University for their help on this project.

## References

[1] Hnatov MV. Incidents, deaths, and in-depth investigations associated with non-fire Carbon Monoxide from engine-driven generators and other engine-driven tools, 1999-2008. Bethesda, MD: U.S. Consumer Product Safety Commission; 2009. p. 16.
[2] CPSC. Portable Generators: Legal Memorandum and staff briefing package for advance notice of proposed rulemaking (ANPR). Bethesda, MD: U.S. Consumer Product Safety Commission; 2006. p. 295.
[3] Hartman J. Nitrous oxide performance handbook: Motorbooks; 2009.
[4] Brown CJ. Engine-drive tools, phase 1 test report for portable electric generators. Bethesda, MD: U.S. Consumer Product Safety Commission; 2006. p. 52.
[5] Persily A, Musser A, Emmerich SJ. Modeled infiltration rate distributions for U.S. housing. Indoor Air. 2010;20:473-85.
[6] Graham LA. Characterizing the cold start exhaust and hot soak evaporative emissions of the test vehicle for the attached garage study. Ottawa: Environment Canada; 1999.
[7] Graham LA, Noseworthy L, Fugler D, O'Leary K, Karman D, Grande C. Contribution of vehicle emissions from an attached garage to residential indoor air pollution levels. Journal of the Air & Waste Management Association. 2004;54:22.
[8] Tsai PY, Weisel CP. Penetration of evaporative emissions into a home from an M85-fueled vehicle parked in an attached garage. Journal of the Air & Waste Management Association. 2000;50:8.
[9] Wang L, Emmerich SJ, Persily AK. In situ experimental study of carbon monoxide generation by gasoline-powered electricity generator in an enclosed space. Journal of the Air & Waste Management Association. 2010;60:19.
[10] Walton GN, Dols WS. CONTAMW 2.4 user manual. Gaithersburg, MD, USA: National Institute of Standards and Technology; 2008. p. 286.
[11] ASTM-E741-00. Standard test method for determining air change in a single zone by means of a tracer gas dilution. West Conshohocken, Pa.: American Society for Testing and Materials; 2006.
[12] NIOSH. Documentation for Immediately Dangerous to Life or Health Concentrations (IDLH): NIOSH Chemical Listing and Documentation of Revised IDLH Values. National Institute for Occupational Safety and Health; 1995.
[13] Bates D, Chambers J, Dalgaard P, Falcon S, Gentleman R, Hornik K, et al. Manuals of the R project for statistical computing. 2.7.2 ed2008.
[14] Swami MV, Chandra S. Correlations for pressure distributions on buildings and calculation of natural-ventilation airflow. ASHRAE Transactions. 1988;94(1):243-66.

[15] Emmerich SJ, Gorfain JE, Huang M, Howard-Reed C. Air and pollutant transport from attached garages to residential living spaces. Gaithersburg, MD: National Institute of Standards and Technology; 2003. p. 28.
[16] ACGIH. Carbon Monoxide. Threshold limit values for chemical substances and physical agents and biological exposure indices. Cincinnati, OH: American Conference of Governmental Industrial Hygienists; 2009.
[17] Levine B. Principles of forensic toxicology: Amer Assn for Clinical Chemistry; 2 edition; 2003.
[18] EPA. Air Quality Criteria for Carbon Monoxide. Washington, DC: U.S. Environmental Protection Agency; 2000. p. 295.
[19] EPA. Proposed acute exposure guideline levels (AEGLS) for Carbon Monoxide. U.S. Environmental Protection Agency; 2001. p. 88.
[20] Peterson JE, Stewart RD. Predicted the carboxy-hemoglobin levels result from carbon monoxide exposure. J Appl Physiol. 1975;39:633-8.
[21] Stewart RD. The effect of carbon monoxide on humans. Annual review of pharmacology. 1975;15:409-23.